Clim Dyn (2011) 37:1869–1887
DOI 10.1007/s00382-010-0976-y

Teleconnections in a warmer climate: the pliocene perspective

Sonali P. Shukla · Mark A. Chandler · David Rind · Linda E. Sohl · Jeff Jonas · Jean Lerner

Received: 3 March 2010 / Accepted: 18 December 2010 / Published online: 4 January 2011
© Springer-Verlag 2010

Abstract Migrations toward altered sea surface temperature (SST) patterns in the Indo-Pacific region are present in the recent observational record and in future global warming projections. These SSTs are in the form of "permanent" El Niño-like (herein termed "El Padre") and Indian Ocean Dipole (IOD)-like patterns. The Early Pliocene Warm Period, which bears similarity to future warming projections, may have also exhibited these Indo-Pacific SST patterns, as suggested by regional terrestrial paleo-climatic data and general circulation model studies. The ability to corroborate this assessment with paleo-data reconstructions is an advantage of the warm Pliocene period that is not afforded by future warming scenarios. Thus, the Pliocene period provides us with a warm-climate perspective and test bed for understanding potential changes to future atmospheric interactions given these altered SST states. This study specifically assesses how atmospheric teleconnections from El Padre/IOD SST patterns are generated and propagate to create the regional climate signals of the Pliocene period, as these signals may be representative of future regional climatic changes as well. To do this, we construct a holistic diagnostic rubric that allows us to examine atmospheric teleconnections, both energetically and dynamically, as produced by a general circulation model. We incorporate KE′, a diagnostic adapted from the eddy kinetic energy generation field, to assess the available energy transferred to these teleconnections. Using this methodology, we found that relative to our Modern Control experiments, weaker atmospheric teleconnections prevail under warm Pliocene conditions, although pathways of propagation still appear directed toward the southwestern United States from our tropical Pacific sector forcing. Propagation directly emanating from the Indian Ocean forcing sector appears to be largely blocked, although indirect teleconnective pathways appear traversing the Asian continent toward the North Pacific. The changes in the atmospheric circulation of Indian Ocean region in response to the underlying specified SST forcing (and indicated by Pliocene paleo-data) may have a host of implications for energy transfer out of and into the region, including interactions with the Asian jet stream and changes to the seasonal monsoon cycle. These interactions warrant further study in both past and future warm climate scenarios.

Keywords Teleconnections · Pliocene · El Padre · Indian Ocean dipole · El Niño

S. P. Shukla (✉)
Deptartment of Earth and Environmental Sciences and the NASA Goddard Institute for Space Studies, Columbia University, New York, NY, USA
e-mail: sps2113@columbia.edu

M. A. Chandler · L. E. Sohl · J. Jonas · J. Lerner
Center for Climate Systems Research, Columbia University, New York, NY, USA

D. Rind
Goddard Institute for Space Studies, National Aeronautics and Space Administration, New York, NY, USA

1 Introduction

Changes in sea surface temperatures (SSTs), particularly in the tropics, impact the overlying atmosphere to create disturbances in the form of "teleconnections" that propagate far downstream (Trenberth et al. 1998 and references therein). This phenomenon has been noted during El Niño events, which affect regional climates as far away as Alaska, the western and eastern United States and areas surrounding the Indian Ocean. Recent analyses of the observational record and of future global warming climate

model simulations have suggested that more permanent changes to the tropical Indo-Pacific SSTs are plausible. These SST changes would be in the form of "permanent" El Niño and Indian Ocean Dipole (IOD)-like patterns. (Permanent changes to the tropical Pacific that mimic El Niño SST patterns are not necessarily related to ENSO processes. Thus, some in the paleoclimate community use the term "El Padre" to describe a year-round El Niño-like Pacific SST state (Ravelo 2008) and we follow this convention here). The consequent changes that these cause to the overlying atmospheric structure and circulation warrant investigation, as this situation may have implications for future regional climatic changes. For example, if the center of convection during a canonical El Niño is permanently present and shifted from its modern mean position (see, e.g., Yeh et al. 2009), it is uncertain whether canonical El Niño-like teleconnections, such as warming over Alaska, increased precipitation over the southern US, and attenuated Indian Ocean monsoons, will occur. Additionally, the current warm-climate projections of a more arid American southwest would be inconsistent with the teleconnections one would expect from El Padre conditions in the Pacific (Meehl et al. 2007). In a warmer world, it is generally possible that strong high-latitude feedbacks will lead to altered zonal and meridional temperature gradients, changing the background state and the way energy travels through the atmosphere.

Paleo-proxy data (Ravelo et al. 2006; Ravelo 2008; Wara et al. 2005) and general circulation model results (Shukla et al. 2009) indicate that El Padre/IOD SST patterns may have manifested during the Warm Pliocene Period (3.3–3.0 million years ago), an interval bearing some similarities to future global warming projections, and marking the last time global temperatures were more than 2°C above twentieth century average values (Molnar and Cane 2002). Furthermore, these SSTs appear to have influenced regional Pliocene temperature and precipitation patterns via atmospheric teleconnections that were altered with respect to today. The ability to corroborate this assessment with paleo-data reconstructions is an advantage of the warm Pliocene period that is not afforded by future warming scenarios. Thus, the Pliocene period provides us with a warm-climate perspective and test bed to understand potential changes to future atmospheric interactions given these altered SST states.

This study specifically assesses how atmospheric teleconnections from El Padre/IOD SST patterns were generated and how they propagated to create the regional climate patterns seen in the warmer Pliocene period. Similar teleconnections may accompany future tropical Indian/Pacific Ocean warming, leading to future regional climate changes that resemble those of the Pliocene world. Modern teleconnection hypotheses involve planetary waves, formed from tropical convection anomalies, that incite robust large-scale climatic changes as they propagate to higher latitudes (Trenberth et al. 1998). Earlier studies tend to focus teleconnection analyses on certain atmospheric attributes, such as height and vorticity, wave activity flux or stream functions. However, when assessing the relationship of large-scale regional climatic changes to remote sea surface temperature (SST) perturbations, a holistic rubric that assesses the origin, movement and magnitude of the teleconnection through a combination of diagnostic quantities provides a more comprehensive characterization of these large-scale features. We utilize the diagnostic fields geopotential height, zonal wind, vorticity, and wave activity, as well as a new diagnostic that looks at the geographic field of baroclinic eddy kinetic energy (KE′), to study the nature of warm climate teleconnections, given altered SST patterns. Such broader analyses of teleconnections will become increasingly important as anomalous heating of the tropical Pacific and Indian Oceans becomes a more frequently occurring pattern, or even a permanent feature, in a globally warmer world.

Our previous study examining the regional Pliocene climates, reviewed in Sect. 2 of this paper, showed the significance of the tropical Indo-Pacific SSTs in correctly simulating the warm Pliocene climate. It also demonstrated the need to understand more fully the nature of warm climate teleconnections. In this paper we describe our diagnostic rubric for analyzing atmospheric teleconnections, taking as an example our experiments that isolate the relative contributions of the Pacific sector El Padre SSTs, the Indian Ocean sector IOD SSTs, and the high latitude warming of the Pliocene. We also describe the results of combined tropical and high-latitude forcings in the Pliocene, and show how warm climate teleconnections of the past and future operate differently compared to modern patterns. Lastly, we discuss the regional implications of warm climate teleconnections, in terms of their significance for the Pliocene, and we offer insights into potential changes in atmospheric interactions across the Indo-Pacific region under future warming conditions.

2 Reproducing warm Pliocene regional climates: a test bed for analyzing teleconnections

Molnar and Cane (2007) suggest that regional mid-Pliocene (annual) temperature and precipitation patterns reconstructed from proxy data resemble those associated with the 1997/1998 El Niño event, which included a strong IOD. In Shukla et al. (2009) we showed that general circulation model simulations which included warm Pliocene boundary conditions combined with a specified El Padre/IOD tropical SST anomaly were better able to reproduce those regional climate patterns than previous model simulations that excluded the altered tropical SST patterns. This

result supports El Padre/IOD SSTs as plausible (permanent) SST configurations in a warmer world.

The Pliocene El Padre/IOD simulation exhibits a strong warming over Alaska that exceeds the degree of Alaskan warming in the Pliocene Control simulation (Fig. 1b, c, respectively). Increased rainfall and cooler temperatures over the southern United States suggest an equatorward shift in the jet stream (Fig. 1c, f). These regional temperature and precipitation responses indicate that the El Padre SST forcing is robust, and that its teleconnections dominate over those from the IOD; any attenuating effect that the IOD teleconnections have on the El Padre forcing is weak from the standpoint of temperature and precipitation. However, the IOD dominates the response in the greater Indian Ocean region, with increased rainfall over East Africa and the Indian sub-continent following the pattern of warm IOD SSTs in the western Indian Ocean basin. It is interesting to note that in the Pliocene Control simulation, where only the high-latitude warming is present, a northward-translated and rotated dipolar precipitation pattern is evident over the Indian sub-continent that is similar to the precipitation pattern forced by the IOD (Fig. 1e). This similarity may indicate a preferred state of the Indian Ocean precipitation response to a warming climate, which must be considered when evaluating the full effect of the El Padre/IOD in our experiments.

Given the reduced meridional temperature gradient in the Pliocene simulation—a decrease of approximately 0.22°C/degree latitude in the Pliocene IOD/El Padre experiment—we expect that circulation mechanisms incited by the anomalous tropical heating could have contributed to the indirect transfer of convective energy out of the tropics. These atmospheric teleconnection mechanisms and their resulting regional climatic patterns have not previously been fully investigated under warm Pliocene boundary conditions. It would appear that the Pliocene background atmospheric circulation and energy transfer related to regional temperature and precipitation patterns differs a great deal from today's. There are three main regions of surface temperature forcings that potentially contribute to the altered atmospheric response: the tropical Pacific Ocean, the tropical Indian Ocean and the large magnitude of high latitude warming. Given these three forcing sources, we suggest holistic diagnostic rubric to assess which regions are contributing most, via atmospheric teleconnections, to these discussed regional climate patterns.

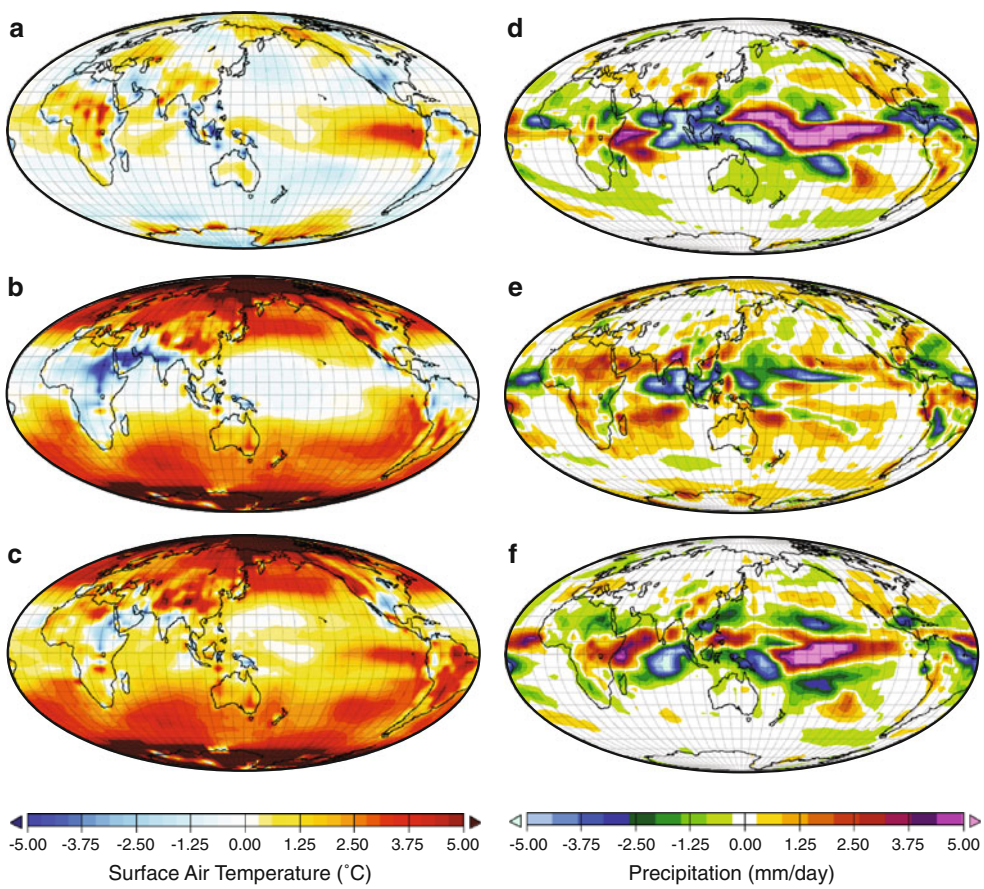

Fig. 1 Annual average surface air temperature anomalies for the **a** Modern El Padre, **b** Pliocene Control, and **c** Pliocene El Padre/IOD simulations. (All anomalies in this and subsequent figures are shown as compared to our Modern Control simulation, unless otherwise stated.) Note the more prominent cooling over the southern USA, and the W-E surface air temperature gradient over the Indian Ocean region in (**a**) and (**c**). Annual average precipitation anomalies for the (**d**) Modern El Padre, **e** Pliocene Control and (**f**) Pliocene El Padre/IOD simulations. The W-E precipitation gradient over the Indian subcontinent is shifted northward in (**e**), in contrast to the more equatorially located W-E precipitation gradient in (**d**) and (**f**)

3 Experiment design and model description

3.1 The GISS global climate middle atmosphere model (GCMAM) version 3

For these studies, we used the GISS Global Climate Middle Atmosphere Model version 3 (hereafter referred to as GCMAM3), which is described in detail by Rind et al. (2007). For these experiments we employ the version with 23 layers in the atmosphere and a top at 0.001 mb (~80 km). GCMAM3, like most GCMs, calculates temperature, pressure, winds, and specific humidity, using the conservation equations for mass, energy, momentum and moisture. The GISS GCMs also use a quadratic-upstream scheme for heat and moisture advection, which implicitly enhances the absolute model resolutions of 4° × 5° (latitude x longitude) to 1.3° × 1.6° (see Schmidt et al. 2006). The radiation physics include all key trace gas constituents (CO_2, CH_4, N_2O, CFCs, and O_3) and aerosols (natural and anthropogenic), and is capable of simulating the effects of large forcing changes in constituents such as volcanic aerosols and greenhouse gases. In addition, a gravity wave drag parameterization incorporates the effects of flow over topography, wind shear and convection. Results from previous versions of the GISS Middle Atmosphere Model are widely published in major scientific studies (e.g., Balachandran and Rind 1995; Shindell et al. 2001; Rind et al. 2001a, b, 2005) and the model has been shown to be robust for extreme paleoclimate scenarios (Rind et al. 2001a).

3.2 GCMAM 3 experimental setup and simulations

Shukla et al. (2009) indicated that the IOD/El Padre state was an important factor in increasing consistency between Pliocene climate model simulations and Pliocene regional climate proxy data. The four simulations presented in this study further investigate how imposed IOD and El Padre SSTs interact with other Pliocene surface temperature forcings and high latitude warming to produce the atmospheric responses that result in the Pliocene regional climate patterns (Table 1).

In order to assess the individual contributions of the Indian Ocean Dipole and a permanent El Niño state to regional climate patterns, two separate simulations (Modern El Padre and Modern IOD) were run, forced by altered tropical Indian and Pacific SST anomalies. The third simulation, our Pliocene Control, investigates the atmospheric response to high-latitude Pliocene warming alone, as specified by boundary conditions prepared by the US Geological Survey's PRISM2 data compilation. The PRISM2 data set for the Pliocene warm period includes global SSTs, vegetation, and ice sheet reconstructions (Dowsett 2007), and reflects high latitude SST warming and reduced sea ice. The fourth and final simulation, Pliocene El Padre, incorporates all three forcings (Pliocene boundary conditions, IOD and El Padre) in order to assess their combined effects in reproducing the regional Pliocene climate patterns. The combined IOD/El Padre SST forcing was obtained by taking the tropical (16°S to 16°N) SST anomaly from November 1997 peak El Niño state and applying it to the Modern and Pliocene boundary conditions. The applied IOD/El Padre anomaly is shown in Fig. 2.

4 Experimental results: teleconnection mechanisms in the Pliocene climate

4.1 Modern teleconnection analyses and their limitations

Convection and vertical motion in the atmosphere balance anomalous heating in tropical regions, leading to high-altitude divergence and subtropical convergence. These divergence/convergence centers can act as a Rossby wave source that emanates directly from the tropics to higher latitudes under westerly background winds. Increases or changes in SSTs are particularly effective at producing wave responses that influence regional climates far from the original center of disturbance. This influence is referred to as a teleconnection, and is inferred to be primary means by which El Niño events impact higher latitudes. As teleconnections move through the atmosphere, they can alter certain characteristics of the atmospheric column, such as temperature, height, and even moisture content, that affect the underlying surface conditions. For example, direct teleconnections emanating from the anomalous El Niño convection center bring cooler, wetter winters to the

Table 1 Description of performed specified sea surface temperature simulations

Simulation name (Specified SSTs)	Simulation description
Modern El Padre	Modern boundary conditions with permanent El Niño (El Padre) SSTs
Modern IOD	Modern boundary conditions with permanent Indian Ocean Dipole (IOD) SSTs
Pliocene control	Pliocene boundary conditions. No additional tropical forcing
Pliocene El Padre/IOD	Pliocene boundary conditions with both permanent El Padre and IOD SSTs

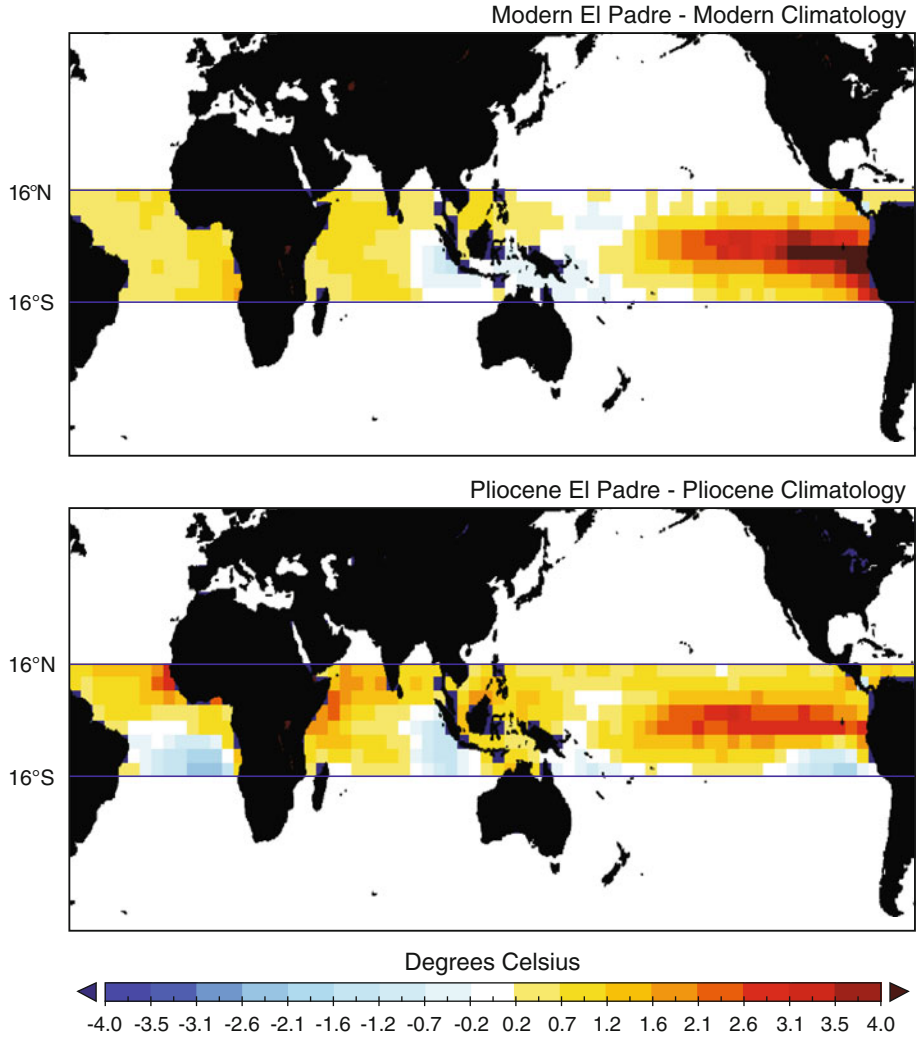

Fig. 2 El Padre and permanent Indian Ocean Dipole (IOD) SST anomalies imposed on specified SSTs between 16°N and 16°S for (**a**) a modern monthly climatology, and (**b**) PRISM2 monthly SST reconstruction

southwestern US and warming to Alaska. When multiple regions experience anomalous SST increases, the waves emanating from these multiple centers may interact downstream. Annamalai et al. (2007) found evidence for this wave interaction by testing both the isolated and combined effects of canonical El Niño SST warming in the central/eastern Pacific, and Indian Ocean (IO) warming. That study found that waves propagating from Indian Ocean SST anomalies directly oppose and destructively interfere with the height anomalies resulting from the tropical Pacific forcing. That is, the waves generated by Pacific and Indian Ocean sectors of tropical warming tend to cancel each other over the North Pacific.

Such tropical SST perturbations can also incite changes in the quasi-stationary features of the mean atmospheric flow. DeWeaver and Nigam (2004) suggested that during El Niño, regions of ocean cooling in the western Pacific, which directly flank the tropical SST increases to the north and south, suppress normal convection. This suppression in turn forces extra-tropical disturbances, such as the relocation of the Pacific jet stream and Aleutian Low. In this case, the anomalous tropical Pacific heating initiates a "chain of causality" that indirectly influences extra-tropical climatic changes. The authors suggest that El Niño teleconnections result not just from the canonical central/eastern tropical Pacific SST warming, but also from contributions of regional cooling anomalies described above.

In the case of warmer climates, even if tropical heating does not produce direct far-reaching teleconnections, indirect impacts may occur at higher latitudes through wave interactions with mid-latitude disturbances and atmospheric flow. Held et al. (1989) theorized that subtropical anomalous convergence forces transients in the vorticity equation via positive vorticity anomalies. Increased eddy kinetic energy generation is a sign of this forcing, with the response manifesting as a planetary wave emanating from the *subtropics* to the northeastern Pacific/Alaskan regions. Additionally, a weaker Walker cell over the tropics induces upper-level easterly flow, which can deflect or absorb equator-bound waves to the extra-tropics,

where the waves' effects would still be felt. As an added example of this indirect teleconnective effect, Hoerling et al. (2004) found that 1950–1999 North Atlantic climatic changes can be partially attributed to warm Indian Ocean SSTs; the North Atlantic response is primarily eddy-driven via adjustment of the storm track, but that adjustment is itself produced by forcing from the Indian Ocean.

It is also possible that tropical-to-high-latitude teleconnections under warmer climates are fully "blocked" owing to non-conducive background zonal flow. Indeed, the atmospheric teleconnection mechanisms themselves may be modified by changes in the background circulation of the Pliocene relative to the modern. Since Rossby wave teleconnections require a strong westerly flow, more direct teleconnections occur during boreal winter when the westerly flow field is strong and conditions are more baroclinic in the lower latitudes. Should the flow become more easterly, the tropical waves are less likely to propagate poleward. Such conditions existed during the strong 1973/74 El Niño event (Ting et al. 1996). Changes to the mid-latitude mean flow via sustained land/sea temperature changes could generate greater stationary wave anomalies at higher latitudes than the forcing by increased tropical SSTs, an occurrence that has been suggested for the 1986/87 El Niño event (Ting and Hoerling 1993).

The study of teleconnections has typically involved identifying strong statistical correlations between SST, or other climatic perturbations, and observed regional climatic changes, and then investigating the direct relationships of the phenomena. In many studies, the teleconnections' source is known or assumed a priori, as is generally the case with El Niño. Teleconnections are then assessed using diagnostics such as geopotential height, vorticity, sea level pressure anomalies or wave propagation metrics, which track the wavetrain from source to regional impact. However, there are some limitations to this approach: examining just one or two diagnostic variables is restrictive because not all aspects of the teleconnection itself are being evaluated, so the typical method of tracking teleconnections may be necessary but not sufficient to understand their sources, evolution, and downstream regional climate impacts. Rather, this minimum number of metrics may just illustrate the teleconnections' local manifestation. These limitations become especially pronounced when the background climatic conditions have been altered (as in the Pliocene), or source for the wave disturbance is not assumed a priori (as is generally the case with modern El Niño studies).

Since the background Pliocene atmospheric flow may itself be altered from modern conditions, we chose to investigate the contribution of three potential sources of altered teleconnections: the tropical Pacific Ocean, the tropical Indian Ocean, and the much warmer high-latitude region of the Pliocene. Geopotential height and vorticity anomalies are useful in tracking wave-like patterns in the atmosphere; consistency between these fields may indicate combined wave propagation from the IOD/El Padre convection centers and any canceling effects between waves from the two sectors. However, they fall short of indicating the source of the teleconnection or the local atmospheric contributions that may modify it. In fact, Branstator (1985) found that "mid-latitude contributions can also change the structure of the wave as some of its components will be amplified and others will not. This has the effect of making the extratropical response favored to some components," a consequence that may not be immediately obvious from analyzing height and vorticity alone. Trenberth et al. (1998) noted that since "small gradients in height can be associated with strong winds in low latitudes," height may not be the most appropriate diagnostic to assess large-scale teleconnections. Likewise, "the z variations (in geopotential height) fail to reveal the tropical circulation changes that often lead to the extratropical wave trains" (Trenberth et al. 1998). The latter point may become a particular concern when there is more than one potential tropical forcing region, as is true for this study.

The development of the wave activity flux (WAF) diagnostic, a three dimensional generalization of the Eliasson Palm Flux, further aids in understanding the trajectory taken by atmospheric waves, and their transfer of energy and momentum (Plumb 1985). To illustrate the modern mean wave propagation field, the WAF and zonal wind field for the Modern control simulation are shown in Fig. 3. Wave propagation extends from the central tropical/subtropical Pacific Ocean to the west coast of the United States, but does not extend from the far western equatorial Pacific to higher latitudes. The eastern Indian Ocean region does show propagation toward the subtropical western Pacific, which then extends across the central subtropical Pacific. The WAF follows the high latitude westerlies over the Asian continent towards Alaska. This diagnostic is useful in assessing stationary wave activity derived from orographic effects, primarily around the Tibetan Plateau and the Himalaya, and from diabatic heating or eddy interaction. However, the WAF diagnostic does not generally show any wave activity propagation from tropical sources, so its use in isolation from other quantities is limited for our simulations, which have two potential tropical teleconnection sources.

Furthermore, when faced with multiple forcing regions for atmospheric teleconnections in addition to Pliocene background conditions, it becomes important to understand where energy is available for wave propagation, and how the wave is modified by additional regional contributions. Local temperature gradients related to land/sea contrasts,

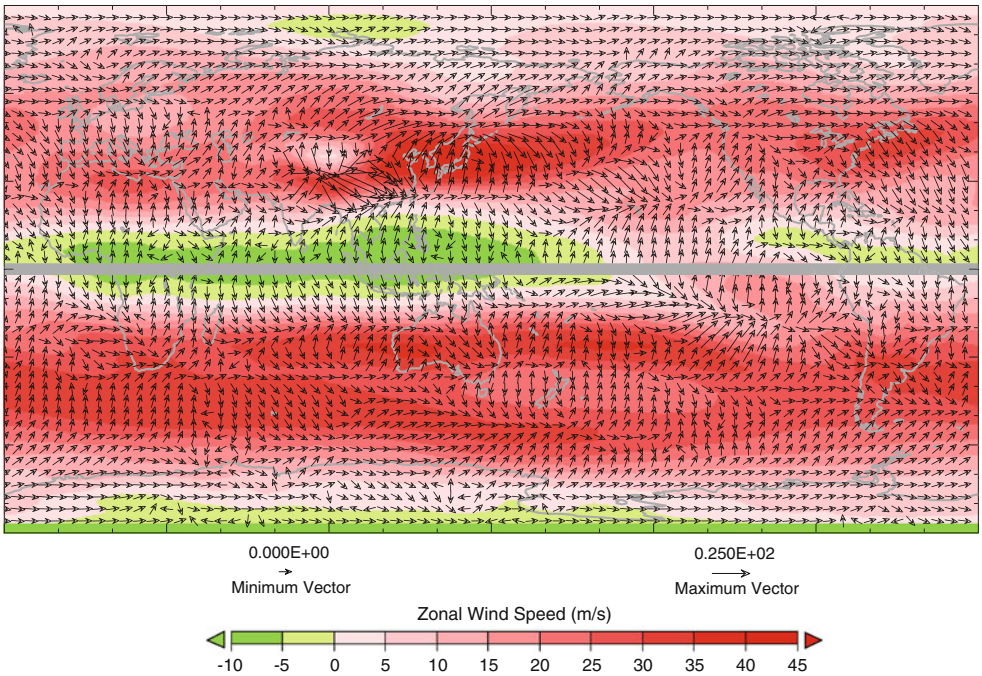

Fig. 3 Annual averaged Modern Control wave activity flux (WAF, shown as vectors; units are 10^{-4} m^2/s^2) and zonal wind field (*green* and *red* shading indicate easterlies and westerlies, respectively). Wave propagation as indicated by the WAF extends from the central tropical/subtropical Pacific Ocean to the west coast of the United States, but does not extend from the western subtropical Pacific or Indian Ocean region to higher latitudes. The eastern Indian Ocean region does show propagation toward the subtropical western Pacific. The WAF follows the high latitude westerlies over the Asian continent towards Alaska. Figures 6, 8 and 10 show the WAF and zonal winds differenced with respect to the Modern Control in order to highlight how these quantities change in our regions of interest, and to give a better picture of each simulation's change in background state

major orographic regions, etc., can modify atmospheric disturbances, and the locations of these gradients in the extra-tropics may have changed under the warm climate conditions of the Pliocene. Branstator (1985) demonstrated the importance of local temperature gradients in linear barotropic simulations of ENSO-type phenomena, noting that "about 40% of the global perturbation KE was derived from this internal source (from local temperature gradients and zonal variations in the jet exit regions) rather than from the tropical heating anomaly." If the position or strength of jet did change under Pliocene conditions, the contribution of the jet to propagating waves, or its presence as a waveguide to tropical disturbances, might have been affected. An assessment of the energetic contribution to the propagating wave, both at its source and along its trajectory, could better address such a situation. This is particularly true along the Asian Jet stream and its interaction with South/Southeast Asian and tropical Indian Ocean disturbances, which can become entrained in the mean jet flow to affect the N. Pacific and northern United States.

In fact, Simmons et al. (1983) found that Pacific perturbations can be generated by forcings located over SE Asia and the tropical NW Pacific. Furthermore, they observe that "wave trains following approximate 'great circle' routes do not necessarily imply a tropical source for the perturbation, and even in the case of tropical forcing the position of the wavetrain does not directly imply the position of the source." An energetic analysis of the teleconnection would better isolate the source and local contributions as the wave moves through the atmosphere, and would better assess the authors' suggestion that the most of the energy supplied to the disturbances emanating from Asia is associated with conversion of mean kinetic energy to eddy kinetic energy.

Lastly, a number of studies (Ting et al. 1996; Ting and Sardeshmukh 1993; Hoskins and Karoly 1981; Held et al. 1989) have highlighted the importance of sub-tropical forcing via high level convergence in response to altered tropical SSTs; the longitudinal positioning of the forcing; the contribution of slow variations of the background; extra-tropical atmospheric circulation; and the extra-tropical eddy contribution to propagating wave activity and its ultimate affect on regional climates downstream. The relative energetic contribution to atmospheric teleconnections by each of these features is not directly ascertained by geopotential height, vorticity, background winds, or the WAF diagnostic alone.

4.2 A dynamic and energetic analysis of atmospheric teleconnections

These limitations led us to construct a diagnostic rubric that would better aid in a more holistic understanding of teleconnections from multiple, combined sources. Through this process, we gain a better understanding of both the energetics and dynamics of the teleconnective mechanism, from source to regional impact. The rubric incorporates the fields of geopotential height, vorticity, zonal winds, wave activity flux, and finally the geographic distribution of the baroclinic eddy kinetic energy generation, calculated as $\omega'\alpha'$.

$\omega'\alpha'$ generation is related to the zonal and local meridional temperature gradients across the tropical Pacific (Fig. 4a, b). The Walker cell is indicated in the rising of warm buoyant air in yellow/red, indicating increased generation, and subsiding warm air in blue, indicating decreased generation, and these motions are corroborated by vertical velocity fields. Kinetic energy generation increases (decreases) may also result from the subsidence (rising) of cold, dense air. Viewing the entire spatial distribution of kinetic energy generation illuminates geographic regions of available energy that contribute to the wave propagation resulting from the specified tropical SST forcing. $\omega'\alpha'$ generation also shows the energy created via the mean zonal (Walker) circulation, and can be used more generally to assess the strength of zonal tropical circulation cells. Generated $\omega'\alpha'$ energy must be available for wave transport, and minimally partitioned to other energy reservoirs, in order to enable tropical-to-extra-tropical teleconnections. These reservoirs include conversions to mean kinetic energy via stronger zonal mean circulation, or conversions to eddy potential energy in the form of local temperature gradients. An intensified (weakened) zonal circulation or increased (decreased) local zonal temperature gradients may indicate less (more) available energy for extra-tropical propagation. Therefore, to make sure that the kinetic energy generated is available for wave transport, the strength of the zonal circulation and local temperature gradients must also be assessed. In our Indian and Pacific Ocean tropical forcing regions, we can further check whether generated $\omega'\alpha'$ energy is potentially available for telconnections by comparing its distribution to the local eddy, or residual, kinetic energy (EKE), which is explicitly calculated from the zonal and meridional wind deviations from the mean. For instance, greater values of EKE occur in the western Pacific (Fig. 4c), where positive $\omega'\alpha'$ generation also exists (Fig. 4b), whereas toward the eastern equatorial Pacific, $\omega'\alpha'$ generation decreases but the EKE increases. If positive $\omega'\alpha'$ generation were to occur in locations of minimal EKE values, this would suggest that the generated energy is potentially available for export by teleconnective waves or it may strengthen the zonal flow, which can be corroborated by mean wind fields discussed above. Should there be a positive correlation between these fields, the generated energy may have been extracted from the zonal circulation or may have been imported by the local convergence of waves, rather than energy being exported to regions far downstream. For the rest of this study, the $\omega'\alpha'$ generation, pictured in Fig. 4b, will be used and termed KE′.

Using all five diagnostic fields of our rubric, we are now able to trace the full path and character of a given teleconnection. The KE′ quantity indicates the energy source available and imparted to the wave for propagation, while the background zonal winds indicate how favorable the source region is (i.e., how strong the westerly background flow is) for both propagation and the transfer of energy to the wave. The wave activity flux (WAF) follows the trajectory, energy and momentum of the wave as it moves through the atmosphere, and indicates the interaction between the anomalous wave energy and the mean flow (as depicted by the zonal winds). Vorticity anomalies indicate if the wave pattern has a local/regional manifestation associated with convergence or divergence of air in the local atmospheric column: negative (positive) vorticity centers are associated with low (high) pressure centers and therefore, positive (negative) height anomalies. The geopotential height anomalies can indicate how stationary features, such as the positions of major troughs and peaks associated with planetary waves, change locales and magnitude with warmer mean climate conditions. Height anomalies are related to the local or regional climate impacts as a result of the transiting wave—these include changes in temperature and precipitation.

4.3 Pliocene teleconnections viewed through a Holistic Rubric

To illustrate the combined utility of the diagnostics in our rubric, we now present the first three simulations from Table 1, which isolate each of the potential surface temperature forcings acting in the Pliocene in order to understand their individual contributions. The combined Pliocene El Padre/IOD simulation is presented in Sect. 4.4, and investigates the interaction between the various forcing components.

4.3.1 Teleconnections from the El Padre SST forcing

A region of increased KE′ is shown over the El Padre forcing region, where warmer SSTs incite greater convective rising motion (Fig. 5a). This finding is confirmed by EKE distributions (not shown), which indicate negative correlation between KE′ and EKE in this region (increases

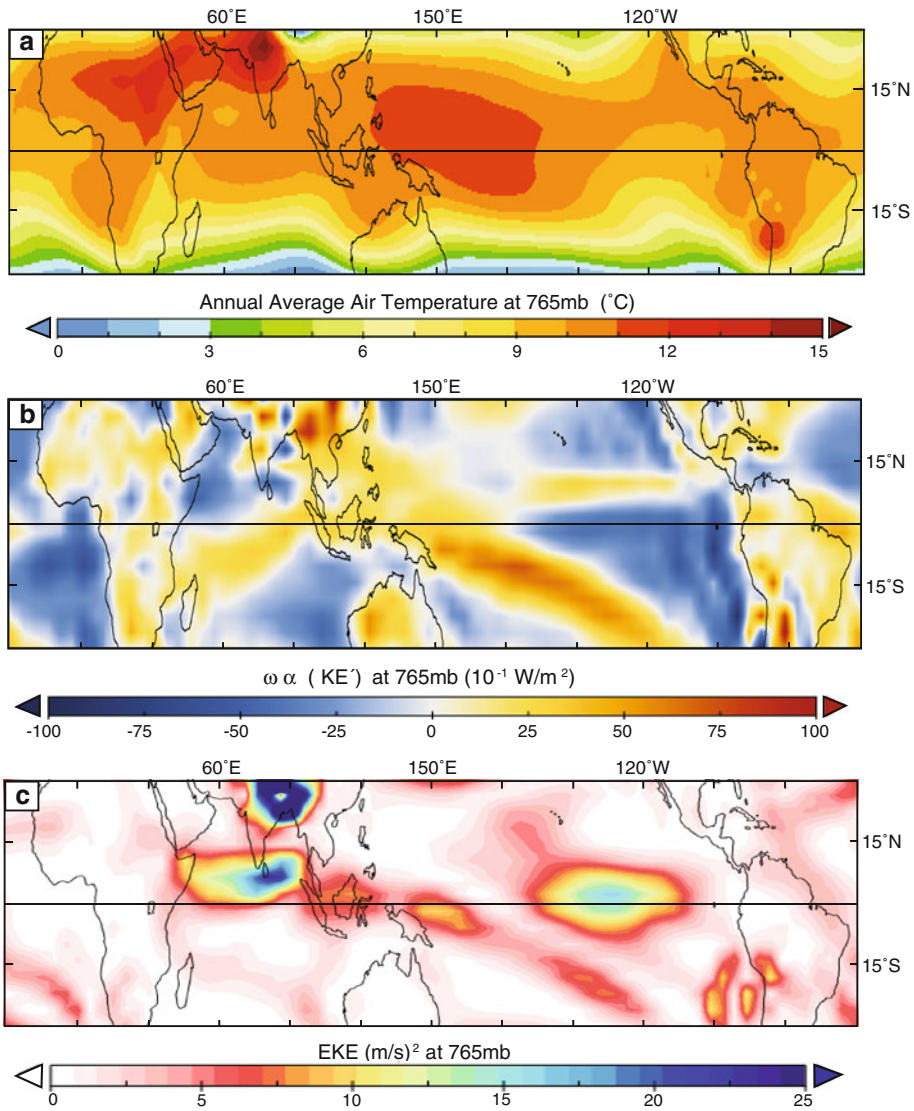

Fig. 4 Comparison of select diagnostics at 765 mb in the tropics of our Modern Control simulation. **a** Annual average atmospheric temperatures indicate the regions of atmospheric temperature gradients that may be energy sources to teleconnections. **b** KE′ (calculated as $\omega'\alpha'$) is increased (decreased) in areas of the tropical western (eastern) Pacific. **c** Eddy kinetic energy (EKE) is calculated from the deviations of the zonal and meridional wind from the mean flow ($\frac{u'^2+v'^2}{2}$); regions of relatively larger values of EKE indicate energy obtained by the zonal flow or imported by converging waves. Regions that have both relative increases in KE′ (Fig. 3b) and decreases in EKE (Fig. 3c) suggest that energy is available for wave propagation

KE′ while EKE decreases), suggesting potential energy export by teleconnections. KE′ decreases occur over most of the tropical western Pacific and Indian Oceans, signifying that less energy is available for propagation from this region. Decreases are shown in the upper level westerly zonal flow over the El Padre forcing region (Fig. 6), while increases in westerly flow appear over the western tropical Pacific and Indian Oceans. Increases in westerlies over the Pacific subtropics indicate a potential equatorward migration of the sub-tropical jet, which can be conducive to wave propagation from a small area of increased KE′ in the western subtropical Pacific. Wave Activity Flux (WAF) patterns (Fig. 6) indicate increased propagation from the subtropical eastern Pacific, north of the El Padre forcing sector. Pathways of propagation north of the El Padre region indicate movement of wave activity towards much of the west coast of the United States, extending into Canada. WAF is also pictured traversing the North Pacific, perhaps following the high latitude mean flow off Asia, to affect portions of Alaska and northern Canada. However, WAF just off the Asian high latitude coast has weakened. WAF from the Indian Ocean region to the high latitudes has weakened. Vorticity (Fig. 5b) indicates negative vorticity centers straddling the El Padre convection center, and positive anomalies (consistent with cooler temperatures) in the lower mid-latitudes over the Southwestern United States. Negative vorticity anomalies (consistent with warmer temperatures) again manifest over Alaska and northern Canada. The whole pattern indicates a wavetrain like response emanating from the tropics. Figure 5c shows height anomalies with expected increases over the forcing region, and decreased height values over the southern

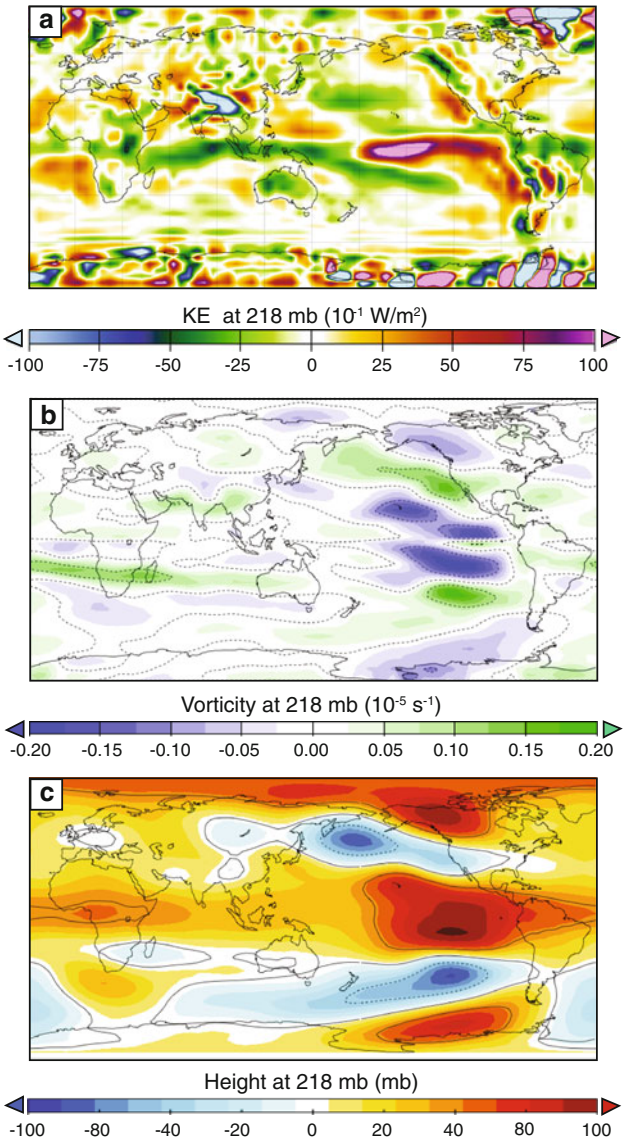

Fig. 5 Modern El Padre—Modern Control annual average anomalies at 218 mb for **a** KE′, **b** vorticity and **c** geopotential height. KE′ increases in **a** occur in the central/eastern equatorial Pacific, the western subtropical Pacific, and off the Californian and Baja coasts. Negative vorticity, **b** anomalies are located over the greater Alaskan region, and positive anomalies are located over the northeastern Pacific and over the southern/southwestern United States. **c** Shows positive height anomalies over greater Alaskan region, and negative height anomalies are located over the northeastern Pacific

United States—a typical symptom of winter El Niño teleconnections, and consistent with increases in precipitation over the region and equatorward shifts in the jet stream. Increased height anomalies are pictured over Alaska and the northeast Pacific, which is consistent with warmer temperatures usually experienced there during El Niño years.

4.3.2 Teleconnections from the IOD SST forcing

Increased KE′ occurs over the western tropical Indian Ocean (Fig. 7a), whereas decreases are shown in the eastern portion of the basin, indicative of a zonal overturning circulation cell much like that of the mean Pacific. Increases in KE′ over the western tropical Indian Ocean and Arabian Sea occur alongside decreases in EKE in the same area (not shown), suggesting energy is available for propagation. Compared to the Modern Control case, the zonal winds indicate slightly stronger easterlies at high levels over the western tropical Indian Ocean (Fig. 3). At low levels (not shown) westerlies prevail over the IOD convection region and easterlies dominate the eastern portion of the basin to converge over the region of increased SSTs. If a zonal overturning cell did manifest over the Indian Ocean, we would expect high-level flow to be more westerly in nature, completing the balance with low-level easterlies converging at the IOD center of convection in the west. More easterly flow over the western Indian Ocean may indicate that KE′ may actually be available for wave propagation, rather than being partitioned into the energy of zonal overturning flow. However, more easterly flow at high levels may also mean that wave activity may not have a background flow conducive to propagation to higher latitudes. Westerly winds anomalies (more conducive to propagation) are depicted over the northern Indian subcontinent. The WAF (Fig. 8) does show propagation from the western Indian Ocean (the IOD convection center) toward higher latitudes. This propagation stream intersects with wave activity around the eastern Himalayan mountain range and the Tibetan Plateau, where WAF increases toward the Northwest Pacific Ocean in a path consistent with the Asian jet. Wave activity on the eastern side of the Indian Ocean is largely blocked and deflected back equatorward. Figure 7b shows a region of negative vorticity over the Arabian Sea, north of the imposed IOD convection center. Positive height anomalies manifest over the northwest Indian/Pakistani region, and alternating patterns in height and vorticity anomalies follow the Asian jet, extending toward the Northeast Pacific/Canadian coast, where it manifests as a positive height/negative vorticity anomaly near Alaska. It should also be noted that positive height anomalies manifest over Southeast Asia and subtropical western Pacific, which could also have an influence over the wave train pattern. Height anomalies (Fig. 7c) from the IOD show wavetrain like propagation from the Arabian Sea towards the Northwest Pacific and downstream. The wave train appears to move toward higher latitudes, showing increased height anomalies over the Northeastern Pacific, and negative height anomalies over Canada. The latter would destructively

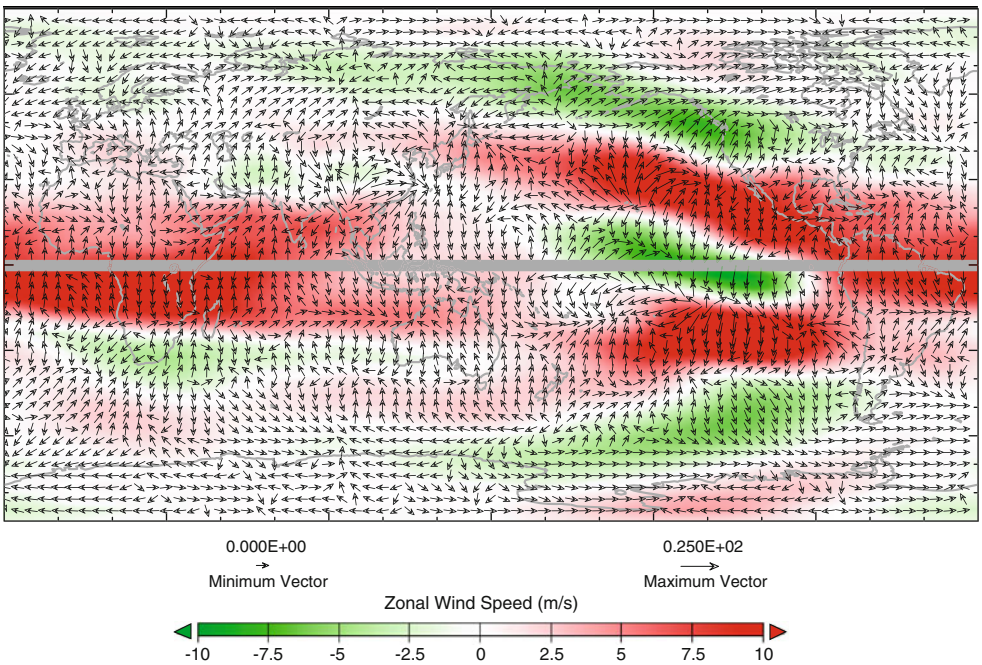

Fig. 6 Modern El Padre—Modern Control anomalies at 218 mb for wave activity flux (WAF, shown as vectors; units are 10^{-4} m^2/s^2) and zonal wind anomalies (*green* and *red* shading indicate easterlies and westerlies, respectively). The WAF indicates increases in eastward propagation paths from the central tropical and eastern subtropical Pacific through the southern US and up to the northeastern Pacific

interfere if imposed directly on top of height anomalies from the El Padre feature.

4.3.3 Teleconnections under high latitude warming (Pliocene control)

The Pliocene Control simulation shows a region of increased KE′ in Fig. 9a over the western tropical Indian Ocean extending to the Arabian Sea and the Indian subcontinent. This occurs with a negative EKE change (not shown), implying that energy is available to propagate from the region. There is also widespread increase in KE′ over the southern Indian Ocean. Further increases in KE′ occur off the coast of Japan and China at higher latitudes. Decreased KE′ is shown around the central and eastern portions of the Indian Ocean basin, extending over the southern Bay of Bengal and Indonesia. The pattern of increased KE′ over the Arabian Sea and decreased KE′ over the Bay of Bengal is similar to that of the Modern Control mean Pacific Walker cell, which could be suggestive of a zonal overturning circulation over the southern Indian peninsula. There is a region of increased KE′ concentrated over the western equatorial Pacific, and decreased KE′ occurring to the west over the Maritime continent.

At mid- and high latitudes, there is a large-scale weakening of the high-level westerly wind field. Easterly anomalies are present everywhere from the sub-tropics up to the higher latitudes. There are confined regions of westerly anomalies over the equatorial central Pacific and southern Indian Oceans. WAF increases from a small region in the eastern tropical Pacific directed towards Mexico and the Southwestern United States (Fig. 10), but across the tropics, propagation to higher latitudes is largely blocked. This is consistent with the large mid-latitude easterly anomalies described above. Propagation within the Indian Ocean is mainly confined to the region, as wave energy propagates equatorward from the Bay of Bengal and Arabian Sea. This suggests that the energy primarily enters the tropical Indian Ocean region from higher latitudes, while little is escaping from the region. There are decreases in wave propagation from the high latitude Asian coast toward the northeast Pacific region.

Figure 9b shows a pair of positive vorticity anomalies straddling a large portion of the central tropical Pacific Ocean that extends to the mid-latitudes. Regions of positive vorticity also manifest over the tropical Northern Indian Ocean, and over the subtropical/mid-latitude southern Indian Ocean. Negative vorticity anomalies appear over the Tibetan Plateau and northern Pacific Ocean, consistent with a heating of the atmosphere in this region. Wave-like patterns from the tropics or subtropics are also not depicted in the height anomalies (Fig. 9c) of the Pliocene, which are largely dominated by the high latitude heating. Negative height anomalies are prevalent in the subtropics, with little change occurring along the equator.

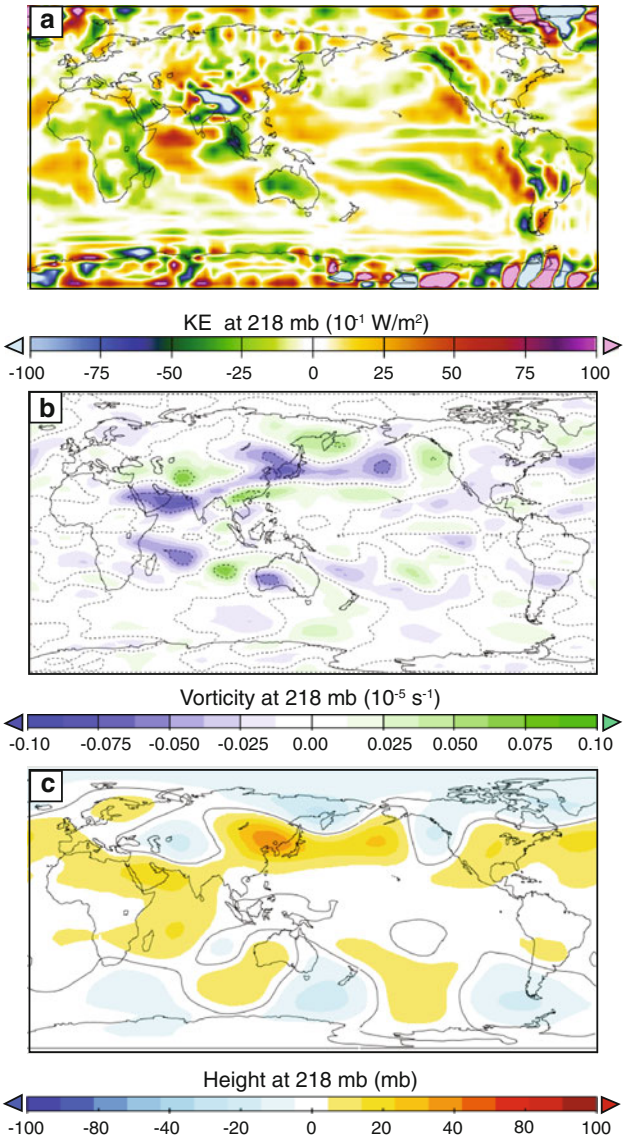

Fig. 7 Modern IOD—Modern Control anomalies at 218 mb for **a** KE′, **b** vorticity and **c** geopotential height. **a** shows KE′ anomalies in the form of zonal overturning over the tropical Indian Ocean. Positive KE′ anomalies prevail over the western tropical Indian Ocean and subtropical western Pacific, whereas decreases occur over the eastern tropical Indian Ocean. Vorticity anomalies, **b** show negative anomalies over the Arabian Sea, north of the IOD forcing. Negative/positive alternating anomalies are pictured extending toward the northeast Pacific Ocean. Geopotential height anomalies, **c** follow a pattern similar to the vorticity, in that positive anomalies prevail over the Indian Ocean region and alternate between negative and positive anomalies extending toward the Northeast Pacific

4.4 Teleconnections from the warm Pliocene IOD/El padre

For regional climates of the Pliocene, when global conditions were considerably warmer, we hypothesize that atmospheric teleconnections of tropical origin had a more indirect influence on extra-tropical regional climates than modern convective events. SST reconstructions indicate decreased meridional temperature gradients, so one possibility is that the Pliocene background wind flow at mid-latitudes behaved more like modern boreal summer conditions, in which westerly flow is weakened, and easterly wind anomalies could refract poleward-bound tropical waves back to the equator and block their energy from reaching higher latitudes. Alternatively, the enhanced tropical heating of the IOD/El Padre state may have generated increased kinetic energy in the subtropics or lower mid-latitudes, which then produced planetary waves affecting climates further poleward. Determining the mechanisms responsible for Pliocene regional climate patterns, and how these mechanisms might relate to modern climate dynamics, requires an analytical approach that is process-oriented rather than statistically-oriented.

KE′ indicates that increased energy is present in the El Padre region of forcing (Fig. 11a). Surface zonal westerly wind anomalies around the El Padre forcing (not shown) indicate decreased tropical zonal circulation, and local temperature gradients remain unchanged from the modern control run, hence there is no increase in local zonal kinetic or available potential energy. Also, as in the modern IOD/El Padre run, there are KE′ increases in the subtropical western Pacific Ocean region. Decreased zonal temperature gradients along the western subtropical Pacific indicate that KE′ generated there may be available for further propagation. However, there are regions of increased zonal local temperature gradients off the Baja peninsula, which indicate that the KE′ generated could be converted to local available zonal potential energy, leaving less energy available for propagation in this region.

Increased KE′ occurs in the Pliocene IOD/El Padre off the coast of Japan and in the northeastern Pacific Ocean basin. Increases in KE′ also occur over Southeast Asia and the Bay of Bengal, as well as over the western Indian Ocean region. Local zonal temperature gradients increase slightly over the greater Tibetan Plateau and are maintained over the Bay of Bengal. The western tropical Indian Ocean, however, does not display local temperature gradient changes between the Pliocene IOD/El Padre and the modern control, and zonal surface circulation (not shown) is greater in the tropical Indian Ocean, indicating that regions of KE′ increase may be strengthening the zonal flow.

The zonal winds in the Pliocene IOD/El Padre run (red and green shading in Fig. 12) indicate a westerly background flow that traverses the mid-latitude Pacific and expands over most of the US. The strongest westerly winds appear off the eastern Asian coastline. Easterly winds, although decreased from the control simulations, prevail in the western tropical Pacific and extend to the central

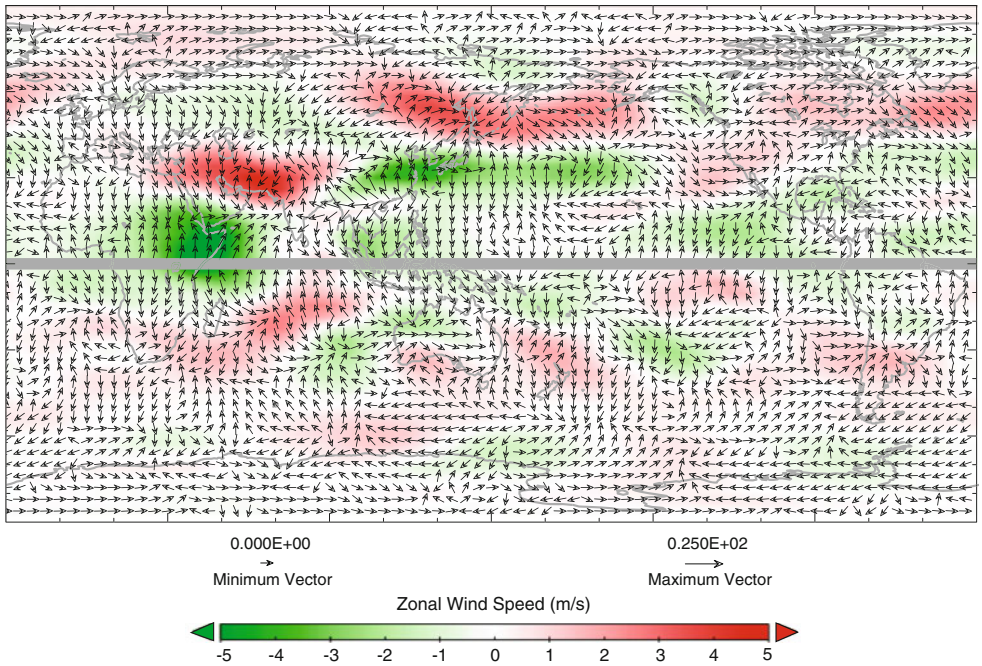

Fig. 8 Modern IOD—Modern Control anomalies at 218 mb for wave activity flux (WAF, shown as vectors; units are 10^{-4} m^2/s^2) and zonal wind anomalies (*green* and *red* shading indicate easterlies and westerlies, respectively). Note the scale difference based upon weaker anomalies depicted in this simulation when compared with Figs. 6 and 10. The WAF indicates a potential indirect propagation from the Arabian Sea (north of the IOD forcing region) toward the convergence over northern India and the Tibetan Plateau. Increases in propagation paths are shown off the Asian coast at high latitudes toward Alaska and the west coast of the United States. Westerly anomalies are present over northern India and the edge of the Tibetan Plateau

Pacific, but they are confined to a narrow meridional band in the eastern tropical Pacific.

With respect to the WAF (vectors in Fig. 12), the Pliocene IOD/El Padre shows pathways propagating from the subtropical western Pacific Ocean along the Asian coastline and Japan, and from over East Asia. These pathways may be supported, in part, by the more confined region of subtropical Pacific and Asian continental KE′ increases shown in Fig. 11a. These western subtropical Pacific/Asian continent wave activity pathways extend across the Pacific to the Bering Straits and greater Alaskan region. However, wave train propagation from the tropics is not consistent with decreases in KE′ that occur over the tropical western Pacific. WAF also appears to be blocked in the tropical Indian Ocean, where easterly winds are prominent. WAF from the eastern/central tropical Pacific propagates toward the northeast through the broad westerly wind field, but is weaker than we see in the modern IOD/El Padre run. The meridional extent of this propagation does not reach the greater Alaskan region, however.

Despite the WAF propagation pathways described above, propagation is generally weaker in the Pliocene IOD/El Padre when compared to the modern control (Fig. 13). As previously described, easterly anomalies (weaker west winds) are present throughout most of the Pacific Ocean region, Asia and the United States. Over the greater Alaskan region, WAF has a strengthened eastward component. However, most of the propagation from the Asian continent displays easterly anomalies, indicating that westerly propagation of WAF has weakened. Propagation strengthens from a southeasterly direction (around the subtropical western Pacific) toward the Himalayas and Tibetan Plateau. WAF from the Indian Ocean region exhibits increased blocking in the modern control, despite slight westerly wind anomalies in the region. Propagation also undergoes blocking from the central/eastern tropical Pacific, despite that region having one of the greatest westerly wind anomalies. Narrow propagation pathways are strengthened from the subtropical eastern/central Pacific and do not encroach upon the west coast of the continental US, but do extend toward the greater Alaskan region. WAF, however, undergoes stronger blocking from the eastern equatorial Pacific Ocean.

Vorticity anomalies depicted in Fig. 11b are not as cohesive in forming definitive wave trains as they are in the Modern El Padre scenario, but weak wave trains can still be discerned. There is a weaker teleconnection pattern, indicated that extends from the subtropical western Pacific Ocean, with contributions from the mid-latitude Asian continent. Weak wave-like disturbances also extend from the central/eastern equatorial Pacific, but these are more zonally elongated, so the wave train itself is less confined to a narrow propagation path than in the modern IOD/El Padre. Height anomalies between the Pliocene El Padre/IOD and modern control simulations are shown in Fig. 11c. Since our imposed boundary conditions are warmer in both the tropics and the higher latitudes with respect to modern conditions, positive height anomalies are prevalent. However, weak wave train-like features are still depicted by less positive height anomalies over the southern United States and subtropical Pacific compared to the tropics or high latitudes. A region of weaker positive height anomalies

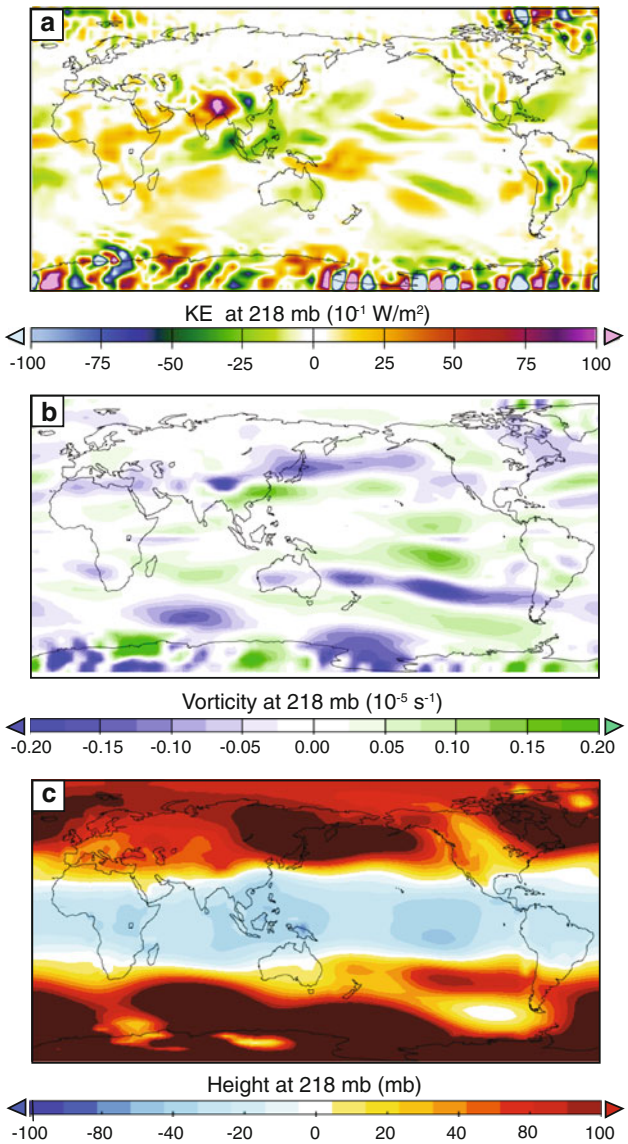

Fig. 9 Pliocene Control—Modern Control anomalies at 218 mb for **a** KE′, **b** vorticity and **c** geopotential height. Increases in KE′, **a** Are shown in the tropical western Pacific Ocean and over the Indian subcontinent and Arabian Sea. Decreases can be seen over the Maritime continent and over the Pacific Ocean in the lower mid-latitudes. Positive vorticity anomalies (**b**) straddle the equator along the central Pacific Ocean and are present over the Pacific lower mid-latitudes. Negative anomalies are shown off the coast of China and Japan and these anomalies extend toward the Pacific Northeast. **c** Shows large height anomalies in the higher latitudes, related to the extreme warming of the high latitudes during the Pliocene period

also appears in the subtropics/lower mid-latitudes of the western Pacific Ocean, with additional wave-like loci occurring over northern Japan and the greater Alaskan region. When the effects of the Pliocene Control simulation are subtracted from the Pliocene IOD/El Padre (not shown), more negative height anomalies are left over the south/southwestern United States, and weak positive height anomalies prevail over Alaska, preserving the El Padre-like climatic patterns in these regions despite the weakened teleconnections.

Furthermore, the seasonal response (not shown) is dominated by wave trains emanating from the western subtropical Pacific and Asian/Indian continent. The (absolute) December–January–February (DJF) response contributes more to the annual average than June–July–August (JJA), as coherent wave train patterns emanate from the subtropical western Pacific and Asian continent during DJF. There is no region of clear, coherent propagation in the JJA response, and all the diagnostics within our rubric are mutually consistent in this result. JJA presents a time of very weak westerly flow in the mid-latitudes, which is not conducive to extra-tropical propagation from the tropics. Stronger westerly zonal winds appear in DJF, enabling energy to be transferred from the western Pacific and Asian continent to the greater northeastern Pacific.

5 Discussion

5.1 Teleconnections: Pacific sector

A permanent El Niño ("El Padre") and Indian Ocean Dipole (IOD), occurring together under otherwise modern climatological conditions, produces annual atmospheric teleconnections over the United States and Canada that resemble those from a canonical El Niño: coherent wave trains emanate from the eastern equatorial Pacific (EEP), affecting the southern United States and northeastern Pacific. Even away from the narrow region of tropical forcing, the teleconnections stay cohesive and robust to much higher latitudes. However, unlike the direct propagation from the EEP, where KE′ was increased, KE′ in the western tropical Pacific decreases and cannot give rise to direct teleconnections. Instead, as the convection center shifts eastward in response to the El Padre SST forcing, the descending branch of the Hadley cell weakens in the west, generating more *subtropical* KE′. Thus, waves emanate from the subtropical western Pacific under El Padre conditions and interact with the mid-latitude mean flow coming off the Asian continent. The energy is, therefore, transferred to the northeastern Pacific by an indirect pathway, but it reaches higher latitudes nonetheless. The resulting climatic impacts are warmer surface air temperatures, positive height anomalies, and negative vorticity anomalies in the North Pacific. Based on our simulations, these two different teleconnection pathways, one originating from the eastern equatorial Pacific and one from the western subtropical Pacific, appear to be characteristic of

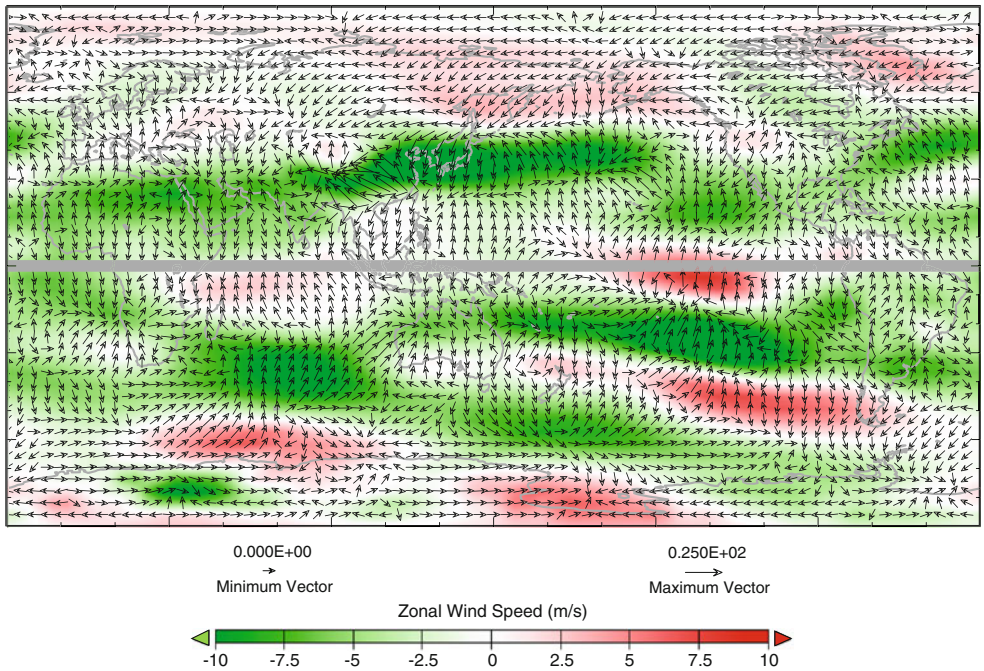

Fig. 10 Pliocene Control—Modern Control anomalies at 218 mb for wave activity flux (WAF, shown as vectors; units are10^{-4} m^2/s^2) and zonal wind anomalies (*green* and *red* shading indicate easterlies and westerlies, respectively). WAF propagation increases from the far eastern subtropical Pacific toward the Baja/Californian coast. Much of the WAF coming tropical Pacific is reduced. WAF from the Indian Ocean region is largely blocked from directly propagating to higher latitudes, but propagation is depicted to strengthen from the subtropical Pacific into western tropical Indian Ocean region. Likewise, WAF propagation from the Asian continent at higher latitudes is weakened and does not penetrate as far eastward (toward the Northeast Pacific) as in the Modern Control

an El Padre state under reduced zonal SST gradient scenarios.

Pliocene climates, on the other hand, have meridional temperature gradients that were greatly reduced compared to modern. We would expect teleconnections of tropical origin to be drastically inhibited, as waves are more likely to travel under stronger temperature gradients and westerly winds (Trenberth et al. 1998). Indeed, in our Pliocene simulation that includes an El Padre SST forcing, the prevalence of easterly zonal wind anomalies makes the possibility of wave activity flux (WAF) to higher latitudes considerably more unlikely than in the modern climate scenario. However, the indirect teleconnections of subtropical origin are produced by the IOD/El Padre forcing even in the warmer Pliocene climate. Overall, the wave trains in the Pliocene are weaker, with all propagation paths from the EEP, the subtropical western Pacific and the Asian continent diminished. Comparisons of the diagnostics in our rubric also indicate that under decreased meridional gradients, as in the Pliocene, the teleconnections themselves are less cohesive as they move through the atmosphere, and are influenced by local and regional disturbances as well as the mean flow.

In our Pliocene simulation, where the specified El Padre SSTs represent a shift of the primary forcing to the central Pacific (see Fig. 1), waves emanating from that region terminate along the southern California coast, as in a modern El Niño scenario. A smaller region of enhanced propagation can also be found extending from the subtropical central Pacific to the northeastern Pacific, though not as far as Alaska. Waves not penetrating to higher latitudes are subject to entrainment in the westerly flow, which ultimately impacts the eastern/northeastern United States. The greater Alaskan region is, however, affected by wave energy traveling via very weakened (with respect to modern) indirect pathways from the western subtropical Pacific and from the Tibetan Plateau/Asian continent, rather than via direct pathways from the central Pacific. Various studies suggest that the center of El Niño convection is migrating toward the central Pacific as the current climate warms (Ashok et al. 2007; Kao and Yu 2009; Yeh et al. 2009), and in addition, northern high-latitude warming is outpacing temperature change everywhere else, so some of our findings for the Pliocene El Padre/IOD may be borne out in future climate impacts.

5.2 Teleconnections: Indian Ocean region

As we have shown, the El Padre in the Pacific basin directly influences the high-latitude response, especially over the northeastern Pacific. This is true for both modern and Pliocene climates. However, this is only one

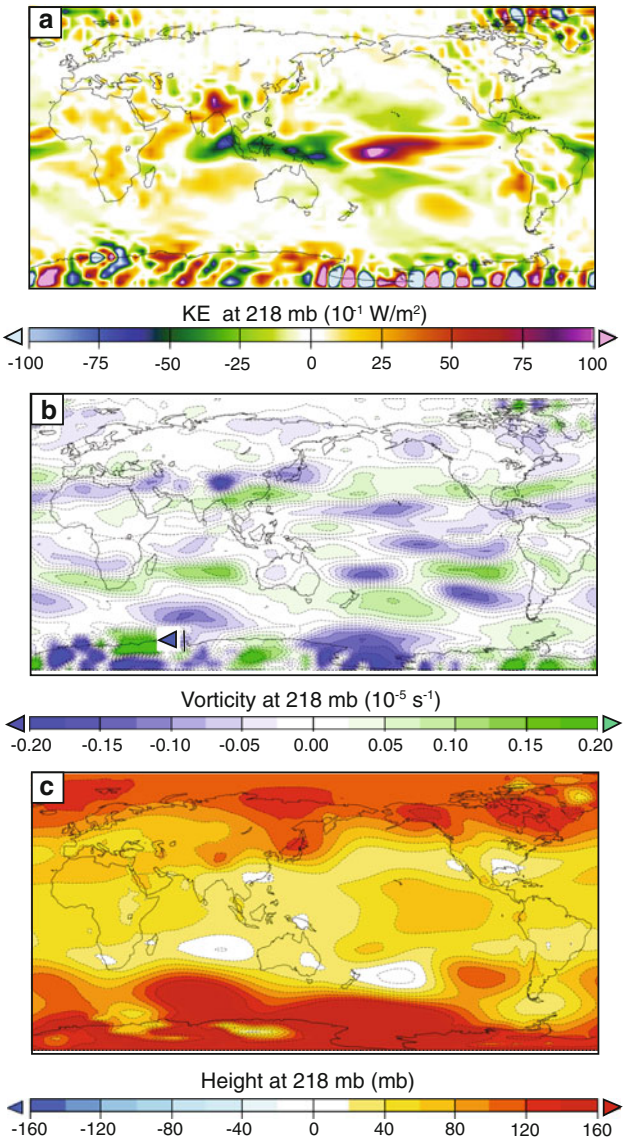

Fig. 11 Pliocene IOD/El Padre—Modern Control anomalies at 218 mb for **a** KE′, **b** vorticity and **c** geopotential height. KE′ increases (**a**) occur in the western tropical Indian Ocean and Arabian Sea and over the central/eastern equatorial Pacific Ocean. Increases are also visible over the subtropical western Pacific Ocean, the Bay of Bengal, and off the coasts of China and Japan. In **b**, negative vorticity anomalies prevail over the central/eastern tropical and subtropical Pacific Oceans, and over much of Alaska. Positive vorticity anomalies occur over the southern United States and Mexico, as well as over most of the Indian subcontinent and Southeast Asia. Negative anomalies occur over the tropical Indian Ocean and off the coasts of China and Japan. **c** Shows positive local height anomalies (relative to the surroundings) over the central/eastern equatorial Pacific and over Alaska. A wave-like pattern of height anomalies is also shown over the southern United States. Height anomalies are greater toward the western portion of the Indian Ocean relative to the east. Local increases in height occur around the Tibetan Plateau and off the coasts of mid-latitude China and Japan

component of the altered tropical SSTs in our experiments; the Indian Ocean Dipole is the other. The Indian Ocean Dipole does not produce direct teleconnections to higher latitudes, but it does have important and direct climatic impacts regionally, in East Africa and over the Indian subcontinent. In both modern and Pliocene climates, easterly winds over the Indian Ocean prohibit wave activity export and so most of the KE′ remains in the region. Any additional KE′ generated under IOD/El Padre forcing conditions goes into strengthening the zonal mean flow. As in the Pacific, there are indirect effects to consider. Interaction between the Indian Ocean Dipole, Himalayan orography and greater Asian circulation patterns modulates waves emanating from the Asian continent, as shown in the patterns of the WAF for our various simulations. This wave activity may combine downstream with subtropical Pacific waves to produce a defined teleconnection transferring tropical energy to higher latitudes.

Another important regional factor is that the presence of an IOD attenuates subsidence over the entire Indian Ocean region, which would otherwise see opposite effects when El Niño-like conditions existed to the east. Additionally, increased kinetic energy generation over the Indian subcontinent could make teleconnections *into* the IO region more feasible, even if energy were not emanating directly *from* the IOD. Results for both modern and warm climates indicate that western subtropical Pacific transfers wave energy to the Indian subcontinent toward the Himalayas, possibly adding to the available energy in the region. KE′ increases are also simulated over the Tibetan Plateau under warm climate conditions, excess energy that may result from the combined warming of the Plateau, the northern Asian continent, and Indian Ocean SSTs. In fact, the high-latitude/Himalaya warming may alone modulate the rainfall over India, producing a dipole-like precipitation pattern even without a forced IOD driving thermal overturning circulation (Fig. 1).

5.3 The Pliocene perspective

IOD/El Padre conditions in the Pliocene simulations yield teleconnections that are supported by terrestrial paleo proxies (Shukla et al. 2009) at locations as far ranging as western North America, the Indian sub-continent, and East Africa. Our simulation results also support the idea, described in detail by Molnar and Cane (2007), that Pliocene proxy data bare a strong resemblance to the impacts of the 1997/98 El Niño. We emphasize, however, that both the IOD and El Padre are needed to fully characterize the Pliocene and provide the best match to terrestrial data, and that this may be an important distinction for a future warm climate as well.

Most evidence now shows that the Pliocene tropical conditions were similar to those we specified using the IOD/El Padre, and the fact that the model simulated El Niño-like teleconnections contrasts sharply with several

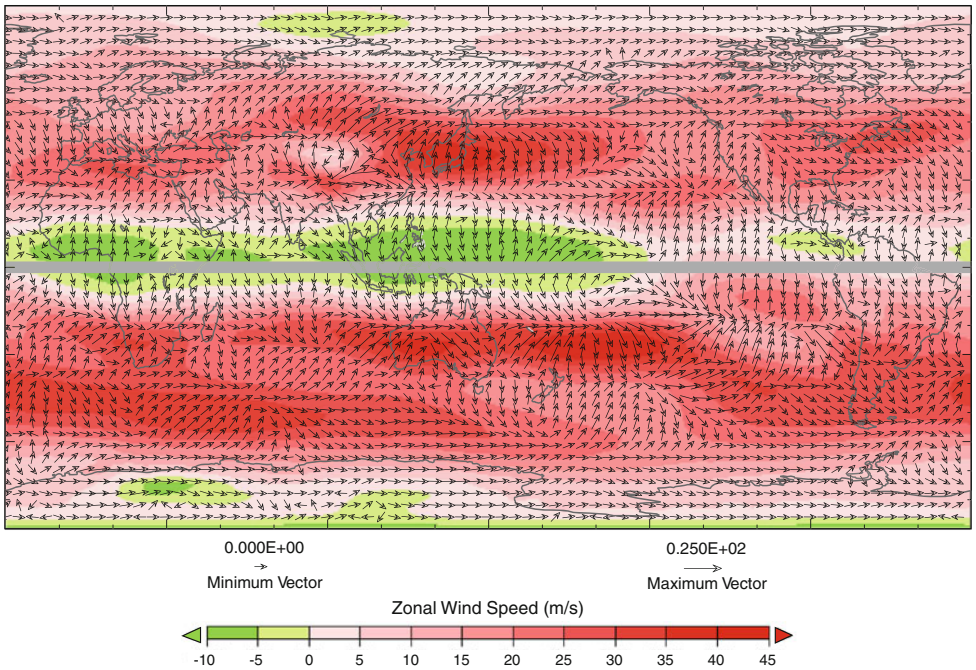

Fig. 12 Pliocene IOD/El Padre annual average zonal wind (*green* and *red* shading indicate easterlies and westerlies, respectively) and wave activity flux (WAF, shown as vectors; units are10^{-4} m^2/s^2) at 218mb. The WAF propagates from the central/eastern Pacific to the southern US and Mexico, but there is no direct a path to the northeastern Pacific. The WAF from the subtropical western Pacific propagates to the northeastern Pacific with contributions from the central Asian continent. Little WAF is shown emanating from the tropical Indian Ocean region to higher latitudes, and zonal wind anomalies in the region are easterly. The tropical Pacific Ocean exhibits easterly anomalies, and most of the WAF from these regions is reduced

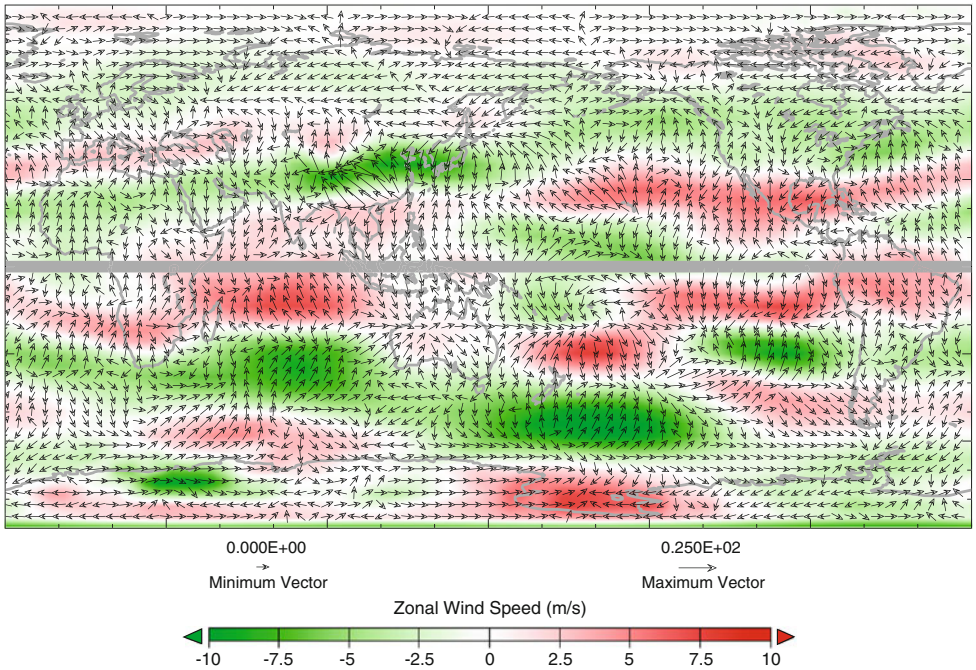

Fig. 13 Pliocene IOD/El Padre—Modern Control anomalies at 218 mb for wave activity flux (WAF, shown as vectors; units are 10^{-4} m^2/s^2) and annual average zonal wind anomalies (*green* and *red* shading indicate easterlies and westerlies, respectively). WAF propagation weakens at most latitudes over the Pacific, along with widespread easterly wind anomalies. Most propagation to the high latitudes is decreased from the EEP. Most WAF is blocked from the Indian Ocean to the high latitudes as easterly wind anomalies occur over the Asian continent

predictions for future climate change. Despite a tendency toward a more El Niño-like state, weak teleconnections, warmer North American temperatures and drying in the American southwest are projected for future climate change (Meehl et al. 2007; Seager et al. 2007; Vecchi and Soden 2007). However, our Pliocene simulations show robust El Niño-like teleconnections to these regions, even with a reduced westerly mid-latitude flow. Increased

rainfall in the Indian Ocean in our results is consistent with future projections and suggests that El Niño will have a waning influence over the region in a future warm climate (Ashok et al. 2001, 2004; Vecchi and Soden 2007). We emphasize that the IOD (or perhaps generally warmer Indian Ocean SSTs) may play a role in this difference, and the complete air-sea interactions between the Indo-Pacific basins in a warmer climate warrants further investigation.

Indeed, the modern interaction between the Indian and Pacific Ocean basins may be subject to change under warm Pliocene conditions. This also holds true for the interaction between oscillatory IOD and El Niño events. These processes are highly coupled atmosphere-land–ocean phenomena, and so it is beyond the scope of this AGCM-only study to comprehensively investigate their interactions or comment on the past or future variability of the IOD and El Niño phenomena. However, prior studies indicate that IOD variability has intensified during the twentieth century as the mean Indian Ocean SSTs have tended toward more positive IOD-like conditions (Abram et al. 2008). This would suggest that permanent alterations in Indo-Pacific SSTs create a more conducive environment for greater IOD and/or El Niño variability (however, this does not suggest causality). Additionally, it is suggested that El Niño conditions in the Pacific favor IOD events in the Indian Ocean, and IOD events may, in turn, interact with El Niño events in the Pacific via both atmospheric and oceanic teleconnections (Izumo et al. 2010). We can imagine a reinforcing scenario in which a permanent reduction in eastern equatorial Indian Ocean SSTs, along with permanent IOD-like overturning atmospheric circulation, favor increased subsidence over the Maritime continent and the western tropical Pacific Ocean. The resulting low level divergence and surface wind forcing could impact the Pacific Walker circulation to reinforce both El Padre and permanent IOD-like SSTs. However, in order to fully assess these mechanisms, the ocean heat transport and dynamic teleconnections must also be considered.

6 Conclusions

Simulations with the GISS GCM indicate that the Indian Ocean Dipole and El Padre conditions have definable impact on tropical and extra-tropical energy transfer. The El Padre, a term indicating a permanent El Niño-like SST state, transfers energy from the tropics to the extra-tropics in both modern and Pliocene climates via direct teleconnections. In the Pliocene, where meridional temperature gradients are greatly reduced, these teleconnections occur through more indirect means and are weakened compared to modern. The Indian Ocean Dipole does not directly transfer energy to the extra-tropics in either modern or Pliocene climates. However, energetic interactions between the western Pacific, the Himalayas and the IOD dominate the regional climatic response, especially precipitation. This emphasizes that studies of both past and future climates need to consider the state of the IOD, together with any El Niño or El Padre, in order to characterize hydrological change across the greater Indian Ocean Region.

Pliocene teleconnections create regional climates that are corroborated by terrestrial paleo proxy data, and differ from future climate projections. These differences manifest in both the magnitude of temperature change and latitudinal distribution of precipitation, where Pliocene regional climates were more similar to those of a canonical El Niño/IOD response than to future climate scenarios. This discrepancy occurs despite the altered (indirect) teleconnection mechanisms described above. Our goal was to use a holistic rubric to evaluate these distinct warm-climate mechanisms both energetically and dynamically. The analysis included an examination of the geographic distribution of baroclinic eddy kinetic energy, which allowed us to identify the energy imparted to teleconnections. This methodology also permitted us to distinguish between direct and indirect pathways of energy transfer, a capability that will be critical for future climate scenarios, where meridional temperature gradients are expected to be diminished and teleconnections altered.

Acknowledgments Funding for this research was provided by the National Science Foundation, ATM-0323516 (to Chandler), and the NASA Climate Program.

References

Abram NJ, Gagan MK, Cole JE, Hantoro WS, Mudelsee M (2008) Recent intensification of tropical climate variability in the Indian Ocean. Nature Geoscience 1:849–853

Annamalai H, Okajima H, Watanabe M (2007) Possible impact of the Indian Ocean SST on the northern hemisphere circulation during El Niño. J Clim 20:3164–3189

Ashok K, Guan Z, Yamagata T (2001) Impact of the Indian Ocean dipole on the relationship between the Indian monsoon rainfall and ENSO. Geophys Res Lett 28:4499–4502

Ashok K, Guan Z, Saji NH (2004) Individual and combined influences of ENSO and the Indian Ocean dipole on the Indian summer monsoon. J Clim 17:3141–3155

Ashok K, Behera SK, Rao SA, Weng H, Yamagata T (2007) El Niño Modoki and its possible teleconnection. J Geophys Res 112:C11007. doi:10.1029/2006JC003798

Balachandran NK, Rind D (1995) Modeling the effects of UV variability and the QBO on the troposphere/stratosphere system. Part I: the middle atmosphere. J Clim 8:2058–2079

Branstator Grant (1985) Analysis of general circulation model sea-surface temperature anomaly simulations using a linear model. Part I: forced solutions. J Atmos Sci 42:2225–2241

DeWeaver E, Nigam S (2004) On the forcing of ENSO teleconnections by anomalous heating and cooling. J Clim 17:3225–3235

Dowsett HJ (2007) The PRISM palaeoclimate reconstruction and Pliocene sea-surface temperature. In: Williams M, Haywood AM, Gregory FJ, Schmidt DN (eds) Deep time perspectives on climate change: marrying the signal from computer models and biological proxies. The Micropalaeontological Society, Special Publications, The Geological Society, London, pp 459–480

Held IM, Lyons SW, Nigam S (1989) Transients and the extratropical response to El Niño. J Atmos Sci 46(1):163–174

Hoerling MP, Hurrell JW, Xu T, Bates GT, Phillips AS (2004) Twentieth century North Atlantic climate change. Part II: understanding the effect of Indian Ocean warming. Clim Dyn 23:391–405

Hoskins BJ, Karoly DJ (1981) The steady linear response of a spherical atmosphere to thermal and orographic forcing. J Atmos Sci 38:1179–1196

Izumo T, Vialard J, Lengaigne M, De Boyer Montegut C, Behera SK, Luo J, Cravatte S, Masson S, Yamagata T (2010) Influence of the state of the Indian Ocean dipole on the following year's El Niño. Nature Geosci 3:168–172

Kao H-Y, Yu J-Y (2009) Contrasting Eastern-Pacific and Central-Pacific types of ENSO. J Clim 22:615–632

Meehl GA, Stocker TF, Collins WD, Friedlingstein P, Gaye AT, Gregory JM, Kitoh A, Knutti R, Murphy JM, Noda A, Raper SCB, Watterson IG, Weaver AJ, Zhao Z-C (2007) Global climate projections. In: Climate change 2007—the physical science basis, contribution of working group I to the fourth assessment report of the IPCC. IPCC, Geneva, pp 749–843

Molnar P, Cane MA (2002) El Niño's tropical climate and teleconnections as a blueprint for pre-ice age climates. Paleoceanogr 17(2):AN1021

Molnar P, Cane MA (2007) Early Pliocene (pre-ice age) El Niño-like global climate: which El Niño? Geosphere 3(5):337–365

Plumb RA (1985) On the three-dimensional propagation of stationary waves. J Atmos Sci 42:217–229

Ravelo AC (2008) Lessons from the Pliocene warm period and the onset of northern hemisphere glaciation. Eos Trans AGU 89(53):PP23E-01

Ravelo AC, Dekens PS, McCarthy M (2006) Evidence for El Niño-like conditions during the Pliocene. GSA Today 16:4–11

Rind D, Demenocal P, Russell GL, Sheth S, Collins D, Schmidt GA, Teller J (2001a) Effects of glacial meltwater in the GISS coupled atmosphere-ocean model: Part I: North Atlantic deep water response. J Geophys Res 106:27335–27354

Rind D, Russell GL, Schmidt GA, Sheth S, Collins D, Demenocal P, Teller J (2001b) Effects of glacial meltwater in the GISS coupled atmosphere-ocean model: Part II: a bi-polar seesaw in Atlantic deep water production. J Geophys Res 106:27355–27366

Rind D, Perlwitz Ju, Lonergan P (2005) AO/NAO response to climate change: 1 respective influences of stratospheric and tropospheric climate changes. J Geophys Res 110:D12107

Rind D, Lerner J, Jonas J, McLinden C (2007) The effects of resolution and model physics on tracer transports in the NASA Goddard Institute for space studies general circulation models. J Geophys Res 112:D09315

Schmidt GA, Ruedy R, Hansen JE, Aleinov I, Bell N, Bauer M, Bauer S, Cairns B, Canuto V, Cheng Y, Del Genio A, Faluvegi G, Friend AD, Hall TM, Hu Y, Kelley M, Kiang NY, Koch D, Lacis AA, Lerner J, Lo KK, Miller RL, Nazarenko L, Oinas V, Perlwitz Ja, Perlwitz Ju, Rind D, Romanou A, Russell GL, Mki Sato, Shindell DT, Stone PH, Sun S, Tausnev N, Thresher D, Yao M-S (2006) Present day atmospheric simulations using GISS ModelE: comparison to in situ, satellite and reanalysis data. J Clim 19:153–192. doi:10.1175/JCLI3612.1

Seager R, Ting MF, Held I, Kushnir Y, Lu J, Vecchi GA, Huang HP, Harnik N, Leetmaa A, Lau NC, Li CH, Velez J, Naik N (2007) Model projections of an imminent transition to a more arid climate in Southwestern North America. Science 316:1181–1184. doi:10.1126/science.1139601

Shindell DT, Grenfell JL, Rind D, Grewe V, Price C (2001) Chemistry-climate interactions in the Goddard Institute for space studies general circulation model: 1. Tropospheric chemistry model description and evaluation. J Geophys Res 106:8047–8076

Shukla SP, Chandler MA, Jonas J, Sohl LE, Mankoff K, Dowsett H (2009) Impact of a permanent El Niño (El Padre) and Indian Ocean dipole in warm Pliocene climates. Paleoceanogr 24:PA2221

Simmons AJ, Wallace JM, Branstator GW (1983) Barotropic wave propagation and instability, and atmospheric teleconnection patterns. J Atmos Sci 40(6):1363–1392

Ting MF, Hoerling MP (1993) Dynamics of stationary wave anomalies during the 1986/87 El Niño. Clim Dyn 9:147–164

Ting M, Sardeshmukh PD (1993) Factors determining the extratropical response to equatorial diabatic heating anomalies. J Atmos Sci 50(6):907–918

Ting M, Hoerling MP, Xu T, Kumar A (1996) Northern hemisphere teleconnection patterns during extreme phases of the zonal-mean circulation. J Clim 9:2614–2633

Trenberth KE, Branstator GW, Karoly D, Kumar A, Lau NC, Ropelewski C (1998) Progress during TOGA in understanding and modeling global teleconnections associated with tropical sea surface temperatures. J Geophys Res 103:14291–14324

Vecchi GA, Soden BJ (2007) Global warming and the weakening of the tropical circulation. J Clim 20:4316–4340. doi:10.1175/JCLI4258.1

Wara MW, Ravelo AC, Delaney ML (2005) Permanent El Niño-like conditions during the Pliocene warm period. Science 309:758–761

Yeh S-W, Kug J-S, Dewitte B, Kwon M-H, Kirtman BP, Jin F-F (2009) El Niño in a changing climate. Nature 461:511–515